JOURNAL OF THE ROYAL SOCIETY Interface

Modelling the checkpoint response to telomere uncapping in budding yeast

C.J Proctor, D.A Lydall, R.J Boys, C.S Gillespie, D.P Shanley, D.J Wilkinson and T.B.L Kirkwood

J. R. Soc. Interface 2007 **4**, 73-90
doi: 10.1098/rsif.2006.0148

JOURNAL OF THE ROYAL SOCIETY Interface

J. R. Soc. Interface (2007) **4**, 73–90
doi:10.1098/rsif.2006.0148
Published online 31 August 2006

Modelling the checkpoint response to telomere uncapping in budding yeast

C. J. Proctor[1,3,*], D. A. Lydall[1,3], R. J. Boys[2,3], C. S. Gillespie[2,3], D. P. Shanley[1,3], D. J. Wilkinson[2,3] and T. B. L. Kirkwood[1,3]

[1]*Institute for Ageing and Health, and School of Clinical Medical Sciences-Gerontology,* [2]*School of Mathematics & Statistics, and* [3]*Centre for Integrated Systems Biology of Ageing and Nutrition, Newcastle University, Newcastle upon Tyne NE4 6BE, UK*

One of the DNA damage-response mechanisms in budding yeast is temporary cell-cycle arrest while DNA repair takes place. The DNA damage response requires the coordinated interaction between DNA repair and checkpoint pathways. Telomeres of budding yeast are capped by the Cdc13 complex. In the temperature-sensitive *cdc13-1* strain, telomeres are unprotected over a specific temperature range leading to activation of the DNA damage response and subsequently cell-cycle arrest. Inactivation of *cdc13-1* results in the generation of long regions of single-stranded DNA (ssDNA) and is affected by the activity of various checkpoint proteins and nucleases.

This paper describes a mathematical model of how uncapped telomeres in budding yeast initiate the checkpoint pathway leading to cell-cycle arrest. The model was encoded in the Systems Biology Markup Language (SBML) and simulated using the stochastic simulation system Biology of Ageing e-Science Integration and Simulation (BASIS). Each simulation follows the time course of one mother cell keeping track of the number of cell divisions, the level of activity of each of the checkpoint proteins, the activity of nucleases and the amount of ssDNA generated. The model can be used to carry out a variety of *in silico* experiments in which different genes are knocked out and the results of simulation are compared to experimental data. Possible extensions to the model are also discussed.

Keywords: systems biology; modelling; stochastic; telomere; checkpoint; yeast

1. INTRODUCTION

Telomeres are repetitive sequences of DNA situated at the ends of linear chromosomes. They require protection from being recognized as double-strand breaks to prevent activation of the DNA damage response. In budding yeast, the telomere-binding protein Cdc13 provides a protective cap at the ends. In the absence of Cdc13, checkpoint proteins bind to the telomeres, resulting in cell-cycle arrest (Weinert & Hartwell 1988; Lydall 2003), accumulation of single-stranded DNA (ssDNA) on the 3′ strands (Garvik *et al.* 1995) and recombination (Grandin *et al.* 2001*a*). A mutant form of Cdc13, *cdc13-1*, has a temperature-dependant response and is only able to cap telomeres at a range of temperatures, with the maximum 'permissive temperature' being 25°C (Garvik *et al.* 1995). At higher temperatures, *cdc13-1* is unable to function, the checkpoint pathway is activated and the cells stop growing. Hence, a temperature in this range is referred to as a 'restrictive temperature'. A useful way to study the checkpoint response in budding yeast is to introduce the *cdc13-1* mutation and to initially culture the cells at a permissive temperature (e.g. 23°C) and then switch to a restrictive temperature (e.g. 36°C). Throughout this paper, we will use the terms permissive temperature and restrictive temperature to refer to *cdc13-1* strains being cultured at 23 and 36°C, respectively. More detail of the experimental framework can be found in Zubko *et al.* (2004).

The end of a telomere in budding yeast consists of a very short region of ssDNA (approx. 12 nt) which is termed an 'overhang' (Larrivee *et al.* 2004). This overhang is usually protected by telomere-binding proteins to prevent it from being seen as DNA damage, which would otherwise activate a DNA damage response. At the restrictive temperature, *cdc13-1* cells possess a small amount of DNA damage, as a result of overhangs becoming exposed, which activates the Rad9- and Rad24-dependent checkpoint pathway. This initial damage is amplified to larger single-stranded regions near telomeres. The generation of ssDNA is a necessary requirement for the full activation of the checkpoint response. There is evidence that the Mrx complex, Exo1 and the Rad24 group regulate or encode nucleases, which are responsible for generating ssDNA at telomeres (Lydall 2003). Exo1 regulates ssDNA levels when telomere capping is defective. For example, Exo1 is essential for ssDNA generation in *yku70Δ* mutants and contributes to ssDNA in *cdc13-1* mutants

*Author for correspondence (c.j.proctor@ncl.ac.uk).

Received 27 June 2006
Accepted 14 July 2006

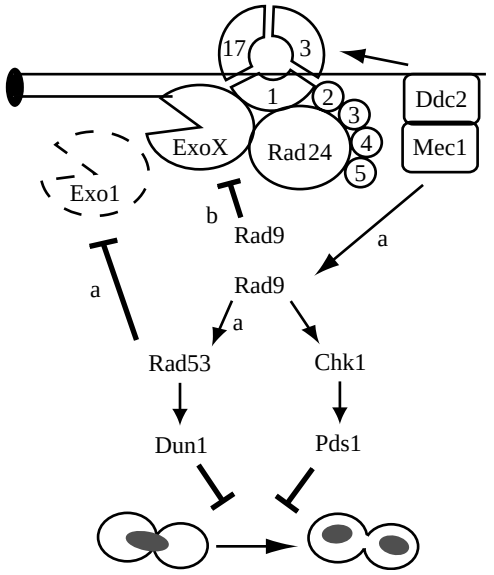

Figure 1. A model for the interaction between checkpoint pathways and nucleases at *cdc13-1*-induced damage (Reproduced with permission from Jia *et al.* (2004), Copyright Genetics Society of America.). Rad9 inhibits ssDNA production at telomeres of *cdc13-1* strains by two routes, a and b. One route, a, depends on Mec1, Rad9 and Rad53 and targets Exo1. The other route, b, is dependent on Rad9, independent of Mec1 and Rad53 and targets ExoX.

(Maringele & Lydall 2002). In *cdc13-1 rad9Δ* mutants, the ssDNA accumulates more rapidly than in *cdc13-1* mutants, whereas in *cdc13-1 rad24Δ* mutants, the ssDNA accumulates much more slowly than in *cdc13-1* cells (Lydall & Weinert 1995). It has been found that ssDNA levels are high in *cdc13-1 rad9Δ exo1Δ* strains, low in *cdc13-1 exo1Δ* strains and low in *cdc13-1 rad53Δ exo1Δ* and *cdc13-1 mec1Δ exo1Δ* strains (Jia *et al.* 2004; Zubko *et al.* 2004). This suggests that Rad9 inhibits an unidentified nuclease called ExoX, and that this inhibition does not require Mec1 or Rad53 (see figure 1).

In order to understand precisely how this important yet complex system of pathways is regulated, there is a clear role for mathematical models. These can help both to reveal gaps and inconsistencies in current knowledge and also to conduct *in silico* experiments (simulations) that can help in the efficient planning of wet experimental studies. A model for the interaction of checkpoint pathways and nucleases at *cdc13-1*-induced damage has been proposed by Jia *et al.* (2004). The model from their paper has been reproduced in figure 1. The Rad17, Mec3 and Dcd1 complex is a heterotrimeric proliferating cell nuclear antigen (PCNA)-type ring, which is loaded onto damaged telomeres by another complex consisting of Rad24 and Rfc2–5 subunits, which together form a clamp–clamp loader system (Majka & Burgers 2003). Once loaded, the Rad17 complex activates ExoX, which generates ssDNA at the telomeres. Mec1 and Ddc2 bind ssDNA independent of the Rad17 complex. Mec1 is essential for phosphorylation and activation of Rad9, which in turn activates two parallel pathways of cell-cycle arrest. One pathway is via the kinase Chk1 and the other pathway is via the kinase Rad53 (Gardner *et al.* 1999; Sanchez *et al.* 1999). Rad9 also inhibits the activity of ExoX (Zubko *et al.* 2004). Exo1 activity is not dependent on Rad24 or Rad17, but its activity is inhibited by Rad53. It has been proposed that Rad9 mediates interactions between the upstream kinase, Mec1 and two parallel downstream kinases, Rad53 and Chk1 (Gilbert *et al.* 2001; Schwartz *et al.* 2002; Blankley & Lydall 2004).

In a study of yeast checkpoint genes, it was found that there was a correlation between the amount of ssDNA and cell death in several single and double mutant strains (Lydall & Weinert 1995). However, more recently it has been found that *mec1Δ*, *rad53Δ* and *exo1Δ* mutations each suppress the rapid loss in viability of *cdc13-1 rad9Δ* mutants, but ssDNA still accumulates (Jia *et al.* 2004). They suggest that ssDNA is only cytotoxic if Mec1, Rad53 and Exo1 convert it into a lethal lesion.

The biochemical mechanisms underlying the DNA damage response are complex and many hypotheses have been put forward to suggest how DNA repair and checkpoint pathways interact. This has motivated us to develop a mathematical model of the system. To build the model, it was necessary to specify precisely each element of the network and its interaction with other elements (see §2.1 for details).

2. THE MODEL

2.1. Elements of the model

The paper describes a core model representing the wild-type from which a number of variants were created to represent a number of experimental knockouts. The set of models, all contain the same network, but the variants have different sets of parameter values or initial conditions. The differences are typically small, but lead to significant variance in phenotype. We use the term 'species' to denote a biochemical entity in the model and interactions between species are referred to as reactions. These terms will be used throughout this paper. The first step in building the model is to define all the species and specify their initial amounts. A complete list for the wild-type variant is given in table 1 and each of the species and all reactions in the model are described later in detail. A complete list of the reactions and their parameters (for the wild-type variant) is given in table 2. We use mass action stochastic kinetics for the rate laws (see Wilkinson 2006 for further details). We also use event structures in our model, which allows species amounts and parameter values to be changed once a particular condition is true. These are detailed in the text and summarized in table 3. Figure 2 shows the reaction network in the model.

2.1.1. Capped telomeres, uncapped telomeres and Cdc13. Budding yeast have 16 chromosomes and hence 32 telomeres in G1, but during S phase, the DNA is replicated resulting in 64 telomeres. To avoid unnecessary complexity, we have omitted detail of DNA replication from this model and assumed that the number of telomeres is constant. The main purpose of this model is to examine the pathways that lead to G2/M arrest and so we have chosen 64 telomeres. Telomeres can be in either a capped or uncapped state

Table 1. Initial conditions for wild-type model.

species	description	systematic name (for genes)[a]	database term[b]	initial value[c] (no. of molecules)
Ctelo	capped telomere	n.a.[d]	GO:0000781	64
Utelo	uncapped telomere	n.a.	GO:0000781	0
Rad17Utelo	uncapped telomere bound by Rad17	n.a.	GO:0000781	0
Cdc13	Cdc13 protein complex	YDL220C	S000002379	300
Rad17	Rad17 protein complex	YOR368W	S000005895	70
Rad24	Rad24 protein complex	YER173W	S000000975	70
RPA	replication protein A	YAR007C, YNL312W, YJL173C	GO:0005662	4000
Mec1	Mec1/Ddc2 complex	YBR136W, YDR499W	S000000340, S000002907	4000
ssDNA	single-stranded DNA (10 nt)	n.a.	n.a.	0
RPAssDNA	ssDNA bound by RPA	n.a.	n.a.	0
Mec1RPAssDNA	RPAssDNA bound by Mec1 complex	n.a.	n.a.	0
ExoXI	inactive ExoX	unidentified	n.a.	70
ExoXA	active ExoX	unidentified	n.a.	0
Exo1I	inactive Exo1	YOR033C	S000005559	670
Exo1A	active Exo1	YOR033C	S000005559	0
Rad9I	inactive Rad9	YDR217C	S000002625	20
Rad9A	active Rad9	YDR217C	S000002625	0
Rad53I	inactive Rad53	YPL153C	S000006074	6900
Rad53A	active Rad53	YPL153C	S000006074	0
Chk1I	inactive Chk1	YBR274W	S000000478	60
Chk1A	active Chk1	YBR274W	S000000478	0
Dun1I	inactive Dun1	YDL101C	S000002259	3000
Dun1A	active Dun1	YDL101C	S000002259	0
ATP	adenosine triphosphate	n.a.	CHEBI:15422	10 000
ADP	adenosine diphosphate	n.a.	CHEBI:16761	1000
recovery	dummy species	n.a.	n.a.	0
sink	dummy species	n.a.	n.a.	0

[a] Systematic names (or open reading frame (ORF)-name) correspond to the stretch of DNA of the sequenced gene.
[b] Database terms starting with: (i) GO are taken from the Gene Ontology database (www.geneontology.org); (ii) S are taken from the *Saccharomyces* Genome Database (www.yeastgenome.org); and (iii) CHEBI are taken from the Chemical Entities of Biological Interest database (www/ebi.ac.uk/chebi/).
[c] Initial amounts of proteins are taken from the yeast GFP fusion database (http://yeastgfp.ucsf.edu).
[d] n.a., not applicable.

and hence we have two species to represent telomeres, which we call Utelo and Ctelo for uncapped and capped telomeres, respectively. We assume that the ssDNA overhangs at the telomere ends are capped by Cdc13. The dissociation rate (the time required for half the protein–DNA complex to dissociate) is approximately 30 min (Lin *et al.* 2001). Cdc13 has a strong binding affinity to single-stranded telomeric DNA with a dissociation constant of *ca* 10^{-7} M (Lin *et al.* 2001). Hence, there is equilibrium between uncapped telomeres (Utelo) and those bound by Cdc13.

$$\text{Utelo} + \text{Cdc13} \rightleftharpoons \text{Cdc13} - \text{Utelo}.$$

To model this equilibrium, we set up two reactions,

$$\text{Utelo} + \text{Cdc13} \xrightarrow{k_1} \text{Ctelo},$$

$$\text{Ctelo} \xrightarrow{k_2} \text{Utelo} + \text{Cdc13},$$

where Ctelo represents the pool of telomeres bound by Cdc13.

The first reaction represents capping and the second reaction uncapping. The capping reaction is a second-order reaction since there are two reactants and is given by k_1[#Utelo][#Cdc13], where '#' represents the number of molecules. The uncapping reaction is a first-order reaction and is given by k_2[#Ctelo]. The value of k_2 can be calculated using information on the time taken for half of the bound Cdc13 to dissociate from the telomere given earlier. Since the biological half-life is given by $t_{1/2} = -\ln(0.5)/\text{degradation rate}$, it follows that $k_2 = -(\ln(0.5)/(30 \times 60))\text{s}^{-1} = 3.85 \times 10^{-4}\ \text{s}^{-1}$. The dissociation constant k_d is 10^{-7} M = 110 molecules per nucleus, assuming that the volume of a yeast nucleus is *ca* 1.8 μm^3 (1.8×10^{-9} µl; http://biochemie.web.med.uni-muenchen.de/Yeast_Biol/). Since $k_d = k_2/k_1$, then $k_1 = 3.6 \times 10^{-6}$ molecule^{-1} s^{-1}. We assume that all the telomeres are in a capped state initially, but there is a dynamic process of uncapping and recapping, hence at any point in time, there is a very low number of uncapped telomeres. Telomeres remain in an uncapped state only very transiently, and signalling proteins do not bind while they are in this transient state.

2.1.2. Binding of uncapped telomeres: Rad17 and Rad24. If a telomere remains uncapped, then the

JOURNAL OF THE ROYAL SOCIETY Interface
JOURNAL OF THE ROYAL SOCIETY Interface

Table 2. Reactions for wild-type model.

reaction	kinetic rate law	reactants	products	parameter	value[a]
capping	k_1[Utelo][Cdc13]	Utelo, Cdc13	Ctelo	k_1	5.0×10^{-4} mol^{-1} s^{-1}
uncapping	k_2[Ctelo]	Ctelo	Utelo, Cdc13	k_2	3.85×10^{-4} s^{-1}
Rad17 binding	k_3[Utelo][Rad17][Rad24][ATP]/(5000 + [ATP])	Utelo, Rad17, Rad24, ATP	Rad17Utelo, Rad24, ADP	k_3	1.5×10^{-8} mol^{-2} s^{-1}
ExoX activation	k_4[ExoXI][Rad17Utelo]	ExoXI, Rad17Utelo	ExoXA, Rad17Utelo	k_4	0.01 mol^{-1} s^{-1}
ExoX activity	k_5[Rad17Utelo][ExoXA]	Rad17Utelo, ExoXA	Rad17Utelo, ExoX-A,ssDNA	k_5	3.0×10^{-4} mol^{-1} s^{-1}
Exo1 activation	k_{6a}[Exo1I]	Exo1I	Exo1A	k_{6a}	5.0×10^{-5} s^{-1}
Exo1 Rad24-dependent activation	k_{6b} [Exo1I][Rad24]	Exo1I, Rad24	Exo1A, Rad24	k_{6b}	5.0×10^{-4} mol^{-1} s^{-1}
Rad17-independent Exo1 activity	k_{7a} [Utelo][Exo1A]	Utelo, Exo1A	Utelo, Exo1A, ssDNA	k_{7a}	3.0×10^{-5} mol^{-1} s^{-1}
Rad17-dependent Exo1 activity	k_{7b} [Rad17Utelo][Exo1A]	Rad17Utelo, Exo1A	Rad17Utelo, Exo1A, ssDNA	k_{7b}	3.0×10^{-5} mol^{-1} s^{-1}
RPA binding1	k_{8a} [ssDNA][RPA]	ssDNA, RPA	RPAssDNA1	k_{8a}	0.001 mol^{-1} s^{-1}
RPA binding 2	k_{8b} [ssDNA][RPAssDNA1]	ssDNA, RPAssDNA1	RPAssDNA2	k_{8b}	100.0 mol^{-1} s^{-1}
RPA binding	k_{8c} [ssDNA][RPAssDNA2]	ssDNA, RPAssDNA2	RPAssDNA	k_{8c}	100.0 mol^{-1} s^{-1}
Mec1 binding	k_{8d}[RPAssDNA][Mec1]	RPAssDNA, Mec1	RPAssDNAMec1	k_{8d}	0.004 mol^{-1} s^{-1}
Rad9 activation	k_9 [Rad9Kin][Rad9I]	Rad9Kin, Rad9I	Rad9Kin, Rad9A	k_9	100.0 mol^{-1} s^{-1}
ExoX inhibition	k_{10a}[Rad9A][ExoXA]	Rad9A, ExoXA	Rad9A, ExoXI	k_{10a}	0.05 mol^{-1} s^{-1}
ExoX Mec1-independent inhibition	k_{10b}[Rad9A][ExoXA]	Rad9I, ExoXA	Rad9I, ExoXI	k_{10b}	0.05 mol^{-1} s^{-1}
Rad53 activation	k_{11} [Rad9A][Rad53I]	Rad9A, Rad53I	Rad9A, Rad53A	k_{11}	10^{-5} mol^{-1} s^{-1}
Chk1 activation	k_{12} [Rad9A][Chk1I]	Rad9A, Chk1I	Rad9A, Chk1A	k_{12}	1.7×10^{-4} mol^{-1} s^{-1}
Exo1 inhibition	k_{13} [Rad53A][Exo1A]	Rad53A,,Exo1A	Rad53A,Exo1I	k_{13}	1.0 mol^{-1} s^{-1}
Dun1 activation	k_{14} [Rad53A][Dun1I]	Rad53A Dun1I	Rad53A, Dun1A	k_{14}	3.3×10^{-6} mol^{-1} s^{-1}
Chk1 cell arrest	k_{15} [Chk1A][G2Mon]	Chk1A, G2Mon	Chk1A G2Moff	k_{15}	0.2 mol^{-1} s^{-1}
Dun1 cell arrest	k_{16} [Dun1A][G2Mon]	Dun1A, G2Mon	Dun1A, G2Moff	k_{16}	0.1 mol^{-1} s^{-1}
release of Mec1 and RPA in S phase	k_{17a} [Mec1RPAssDNA][S]	Mec1RPAssDNA, S	3ssDNA Mec1, RPA, S	k_{17a}	0.05 mol^{-1} s^{-1}
release of Mec1 and RPA in G2/M arrest	k_{17b} [Mec1RPAssDNA][G2Moff]	Mec1RPAssDNA, G2Moff	3ssDNA Mec1, RPA, G2Moff	k_{17b}	0.05 mol^{-1} s^{-1}
removal of ssDNA in S phase	k_{18a} [ssDNA][S]	ssDNA, S	S	k_{18a}	0.001 mol^{-1} s^{-1}
removal of ssDNA in G2/M arrest	k_{18b} [ssDNA][G2Moff]	ssDNA, G2Moff	G2Moff	k_{18b}	1×10^{-5} mol^{-1} s^{-1}
recovery	k_{19} [Rad17Utelo][Cdc13][recovery]	Rad17Utelo, Cdc13, recovery	Ctelo, Rad17, recovery	k_{19}	0.001 mol^{-2} s^{-1}

[a] mol, number of molecules.

Table 3. Summary of events used in all models.

event	trigger	species affected	parameters affected	reactions affected
Rad9 kinase activation	Mec1RPAssDNA > 800	Rad9Kin	none	Rad9 activation
ssDNA removal	Mec1RPAssDNA + RPAssDNA + ssDNA < 1	recovery	none	recovery
G2/M recovery completed	Rad17Utelo == 0 && G2 == 1	G2Moff, G2Mon, recovery, ExoXA, ExoXI, Exo1A, Exo1I, Rad9A, Rad9I, Rad53A, Rad53I, Chk1A, Chk1I, Dun1A, Dun1I	none	all reactions involving ExoX, Exo1, Rad9, Rad53, Chk1, Dun1. Recovery reaction stops
S phase recovery completed	Rad17Utelo == 0	recovery	none	recovery
cell death[a]	Mec1RPAssDNA + RPAssDNA + ssDNA > 2000	none	k_{alive}[b]	all reactions stop

[a] Only in models with cell death.
[b] k_{alive} is a parameter which is included in all the kinetic rate laws (e.g. $k_{\text{alive}} \times k_2$[Ctelo]). Initially, $k_{\text{alive}} = 1$ and so rate laws are unaffected by this parameter. When the critical threshold of total single-stranded DNA is reached k_{alive} is set to 0, and so all the reaction rates are equal to 0.

Rad17 complex is loaded onto the telomere end by the Rad24 clamp loader complex. This loading requires ATP and can be represented by the biochemical reaction

$$\text{Utelo} + \text{Rad17} + \text{Rad24} + \text{ATP} \xrightarrow{k_3} \text{Rad17Utelo} + \text{Rad24} + \text{ADP},$$

where Rad17Utelo represents the binding of Rad17 to the telomere end. For simplicity, we have omitted details of Mec3 and Ddc1 in the Rad17 complex and omitted the Rfc2–5 subunits in the Rad24 complex, since they are unimportant for this model. Since there are four reactants in the Rad17-binding reaction, the stochastic rate law is a fourth-order reaction. Care needs to be taken when considering higher order reactions. For example, it is not realistic that the reaction rate would increase indefinitely with an increase in ATP levels; doubling the level of ATP in the cell would not necessarily double the reaction rate. Instead, we would expect that the reaction rate would increase asymptotically with ATP levels. Therefore, we use the rate law k_3[#Utelo][#Rad17][#Rad24][#ATP]/(5000+[#ATP]).

The term in the denominator ensures that the reaction rate increases approximately linearly with ATP when ATP levels are low (less than *ca* 2000), but for high levels of ATP (greater than 5000), the increase in the reaction rate starts to level off with increasing ATP levels. The value for k_3 was chosen by making an initial estimate and then simulating the model and comparing output to the experimental data. Further details of how we chose parameter values can be found in §2.3.

When Cdc13 is present, this reaction is very unlikely to occur as the binding strength of Rad17 compared to Cdc13 is extremely low. However, in the absence of Cdc13, this reaction will eventually take place and an irreversible set of reactions is initiated leading to the generation of ssDNA and cell-cycle arrest unless the pathway is interrupted downstream. We chose a very low value for k_3, to ensure that the probability of a telomere, which is only transiently uncapped, binding to Rad17 is very low.

2.1.3. Nuclease activity: ExoX, Exo1 and ssDNA. ExoX is recruited to telomeres bound by Rad17, and degrades one of the strands to leave a long stretch of ssDNA. This reaction can only occur if ExoX is in its active state. The binding of telomeres by Rad17 (which in turn requires Rad24) is required for ExoX activation. This can be represented simply by the following reactions:

$$\text{ExoXI} + \text{Rad17Utelo} \xrightarrow{k_4} \text{ExoXA} + \text{Rad17Utelo}$$

$$\text{Rad17Utelo} + \text{ExoXA} \xrightarrow{k_5} \text{Rad17Utelo} + \text{ExoXA} + \text{ssDNA},$$

where ExoXI represents the inactive form of ExoX and ExoXA represents activated ExoX. We assume that each time this reaction takes place, 10 nt ssDNA are produced and we set one unit of ssDNA equal to 10 nt. The reaction can continue to take place until ExoX is inactivated. It has been observed that *ca* 8 kb ssDNA

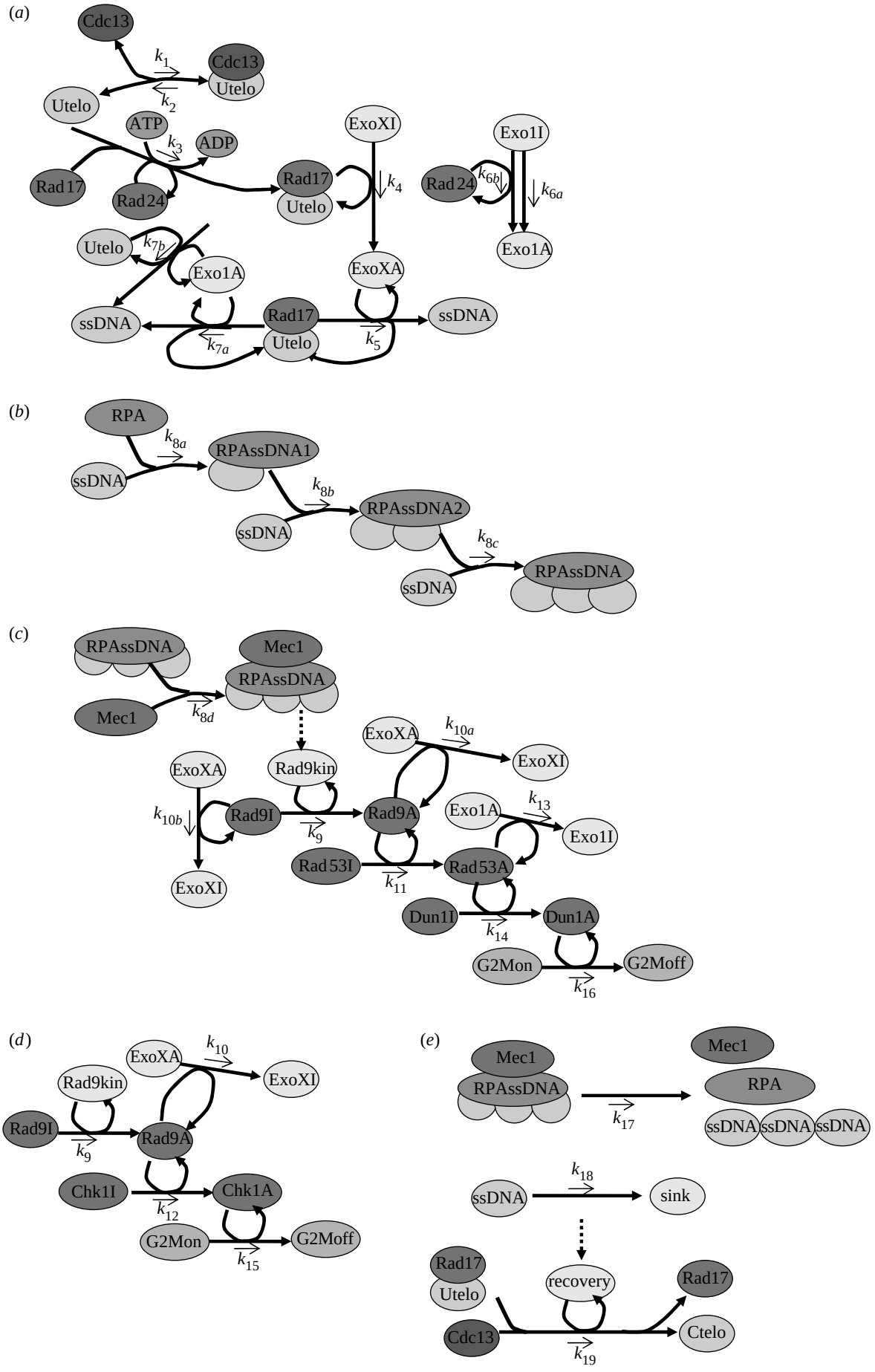

Figure 2. (*Caption opposite.*)

Figure 2. (*Opposite.*) Network diagram showing the checkpoint response to uncapped telomeres. (*a*) Activation of ExoX and Exo1. ExoX requires Rad24 and Rad17 binding for its activation. Exo1 is activated independent of Rad24 and Rad17, although it may also act on telomeres bound by Rad17 and be activated in a Rad24-dependent manner. (*b*) Binding of single-stranded DNA (ssDNA) by RPA. Each molecule of RPA requires three units of ssDNA to bind. (*c*) Activation of checkpoint response via Rad53/Dun1 pathway. Activation of this pathway leads to inhibition of nuclease activity. Dashed line indicates an event, where a threshold level of Mec1RPAssDNA activates a kinase (Rad9Kin) which activates Rad9. (*d*) Activation of checkpoint response via Chk1 pathway does not affect Exo1. (*e*) Recovery can take place during S phase or G2/M arrest after single-stranded DNA has been removed. The dashed line indicates an event. When the level of ssDNA is equal to 0, the dummy species 'recovery' is set to 1 and the recapping reaction can then occur. See §2.1.6 for more details.

are generated in 1 h in *cdc13-1* strains (Jia *et al.* 2004; Zubko *et al.* 2004). Exo1 degrades not only unprotected telomeres, independent of ExoX and Rad17, but also telomeres bound by Rad17. Exo1 activation does not require Rad24. Since *cdc13-1 rad24Δ* mutants have low levels of ssDNA (Lydall & Weinert 1995), we assume that activation of Exo1 is much lower than that of ExoX. There are very low levels of ssDNA in the *cdc13-1 rad24Δ* strain, which must be due to Rad24-independent activation and subsequent activity of Exo1. However, the difference between the amounts of ssDNA in *cdc13-1 exo1Δ* compared to *cdc13-1* mutants is large (Zubko *et al.* 2004), suggesting that Exo1 activity is higher when Rad24 is present. Therefore, we also include an additional reaction of Rad24-dependent activation of Exo1, although this was not in the model proposed by Jia *et al.* (2004) (see figure 1). The reactions for nuclease activity are as follows:

$$\mathrm{Exo1I} \xrightarrow{k_{6a}} \mathrm{Exo1A},$$

$$\mathrm{Exo1I} + \mathrm{Rad24} \xrightarrow{k_{6b}} \mathrm{Exo1A} + \mathrm{Rad24},$$

$$\mathrm{Utelo} + \mathrm{Exo1A} \xrightarrow{k_{7a}} \mathrm{Utelo} + \mathrm{Exo1A} + \mathrm{ssDNA},$$

$$\mathrm{Rad17Utelo} + \mathrm{Exo1A} \xrightarrow{k_{7b}} \mathrm{Rad17Utelo} + \mathrm{Exo1A} + \mathrm{ssDNA}.$$

2.1.4. Binding of ssDNA: replication protein A and Mec1. Replication protein A (RPA) binds to ssDNA with every molecule of RPA binding to 30 nt ssDNA (Zou & Elledge 2003). As each unit of ssDNA is equivalent to 10 nt, we assume that one molecule of RPA binds to three units of ssDNA. Mec1 in complex with Ddc2 then binds to RPA (Zou & Elledge 2003). Thus, binding of ssDNA can be represented by the following two reactions:

$$3\mathrm{ssDNA} + \mathrm{RPA} \xrightarrow{k_{8a}} \mathrm{RPAssDNA},$$

$$\mathrm{RPAssDNA} + \mathrm{Mec1} \xrightarrow{k_{8b}} \mathrm{Mec1RPAssDNA}.$$

Since three units of ssDNA are required for the RPA-binding reaction, the mass action stochastic kinetic rate law is given by k_{8a}[#RPA][#ssDNA][#ssDNA-1][#ssDNA-2]/6. However, this rate law is only valid if the ssDNA units are independent. This is certainly not the case, and the rate law should be a linear and not a cubic function of the total amount of ssDNA. Therefore, we model RPA binding as a series of steps. To do this, we introduce two dummy species RPAssDNA1 and RPAssDNA2 for the intermediate steps. In the first step, RPA binds to one unit of ssDNA to form RPAssDNA1. The rate of this reaction depends linearly on the total amount of ssDNA. In the next step, RPAssDNA1 binds to the second unit of ssDNA to form RPAssDNA2 and finally RPAssDNA2 binds to the third unit of ssDNA to form RPAssDNA. Once the first step has happened, the next two steps follow quickly by setting the rate constants to a high value ($k_{8b}=k_{8c}=100$). The full set of reactions for RPA and Mec1 binding are

$$\mathrm{ssDNA} + \mathrm{RPA} \xrightarrow{k_{8a}} \mathrm{RPAssDNA1},$$

$$\mathrm{ssDNA} + \mathrm{RPAssDNA1} \xrightarrow{k_{8b}} \mathrm{RPAssDNA2},$$

$$\mathrm{ssDNA} + \mathrm{RPAssDNA2} \xrightarrow{k_{8c}} \mathrm{RPAssDNA},$$

$$\mathrm{RPAssDNA} + \mathrm{Mec1} \xrightarrow{k_{8d}} \mathrm{Mec1RPAssDNA}.$$

2.1.5. Checkpoint activation: Rad9, Rad53, Chk1 and Dun1. A very large threshold of *ca* 10 kb ssDNA is required for keeping checkpoints active in order to maintain cell-cycle arrest (Vaze *et al.* 2002; Zubko *et al.* 2004; Maringele & Lydall 2005). To prevent activation of Rad9 when only low levels of ssDNA are present, we modelled this activation as a two-step process. First, we used an event structure in the model to activate a kinase that activates Rad9 (called 'Rad9Kin'), if the total amount of ssDNA within the cell exceeded 8 kb. The rate for the Rad9-activation reaction is equal to k_9[#*Rad9I*][# *Rad9Kin*] and will be equal to 0 as long as Rad9Kin = 0. Once Rad9Kin is activated (so that Rad9Kin = 1), the Rad9-activation reaction can proceed. The event and reaction representing Rad9 activation are as follows:

$$\text{If } \mathrm{Mec1RPAssDNA} > 800, \quad \mathrm{Rad9Kin} = 1,$$

$$\mathrm{Rad9Kin} + \mathrm{Rad9I} \xrightarrow{k_9} \mathrm{Rad9Kin} + \mathrm{Rad9A}.$$

Activated Rad9 activates both Rad53 and Chk1. Rad53 in turn, inhibits the activity of Exo1 and activates Dun1. Rad9 also inhibits ExoX. This inhibition does not require Rad9 to be activated by Mec1 and so it is represented by two reactions, one with Rad9I and the other with Rad9A

$$\mathrm{Rad9A} + \mathrm{ExoXA} \xrightarrow{k_{10a}} \mathrm{Rad9A} + \mathrm{ExoXI},$$

$$\mathrm{Rad9I} + \mathrm{ExoXA} \xrightarrow{k_{10b}} \mathrm{Rad9I} + \mathrm{ExoXI},$$

$$\mathrm{Rad9A} + \mathrm{Rad53I} \xrightarrow{k_{11}} \mathrm{Rad9A} + \mathrm{Rad53A},$$

$$\mathrm{Rad9A} + \mathrm{Chk1I} \xrightarrow{k_{12}} \mathrm{Rad9A} + \mathrm{Chk1A},$$

$$\mathrm{Rad53A} + \mathrm{Exo1A} \xrightarrow{k_{13}} \mathrm{Rad53A} + \mathrm{Exo1I},$$

$$\mathrm{Rad53A} + \mathrm{Dun1I} \xrightarrow{k_{14}} \mathrm{Rad53A} + \mathrm{Dun1A}.$$

Activation of Chk1 and Dun1 results in G2/M arrest

$$\text{Chk1A} + \text{G2Mon} \xrightarrow{k_{15}} \text{Chk1A} + \text{G2Moff},$$

$$\text{Dun1A} + \text{G2Mon} \xrightarrow{k_{16}} \text{Dun1A} + \text{G2Moff},$$

where G2Mon and G2Moff are dummy species, which control whether the cell cycle can progress from G2 to M. If G2Mon = 1 and G2Moff = 0, then the above reactions can occur. If G2Mon = 0 and G2Moff = 1, then the reactions cannot take place (see appendix A for details of modelling the cell cycle).

2.1.6. Recovery. The ssDNA may be removed during S phase by DNA replication. It is also possible that ssDNA is removed during G2/M arrest. When all the ssDNAs have been removed, the uncapped telomeres can be recapped by Cdc13 and recovery takes place. After recovery, all the checkpoint proteins are turned off and cell division can take place. This procedure is modelled by a series of reactions and events

$$\text{Mec1RPAssDNA} + \text{S} \xrightarrow{k_{17a}} 3\text{ssDNA} + \text{Mec1} + \text{RPA} + \text{S},$$

$$\text{Mec1RPAssDNA} + \text{G2Moff} \xrightarrow{k_{17b}} 3\text{ssDNA} + \text{Mec1} + \text{RPA} + \text{G2Moff},$$

$$\text{ssDNA} + \text{S} \xrightarrow{k_{18a}} \text{S},$$

$$\text{ssDNA} + \text{G2Moff} \xrightarrow{k_{18b}} \text{G2Moff}.$$

If Mec1RPAssDNA + RPAssDNA + ssDNA = = 0, then recovery = 1 (where 'recovery' is a dummy species in the model).
If recovery = 1, then the following reaction can proceed:

$$\text{Rad17Utelo} + \text{Cdc13} + \text{recovery} \xrightarrow{k_{19}} \text{Ctelo} + \text{Rad17} + \text{recovery}.$$

If Rad17Utelo = 0 (i.e. all telomeres have been recapped), then G2Moff is set to 0, G2Mon is set to 1, recovery is set to 0, and all other checkpoint proteins are reset to their initial conditions. A network diagram of the full system is shown in figure 2.

2.2. The cell cycle

We also include a series of reactions to represent the different stages of the cell cycle (see appendix A). We assume that ssDNA can be removed by DNA replication when the cell is in S phase and also to a lesser extent when cells are in G2/M arrest. Although it is unclear whether DNA replication can take place in G2/M arrest, it has been observed that the level of ssDNA does decrease in cells, which are arrested (Jia *et al.* 2004; Zubko *et al.* 2004). When budding yeast divides, the mother cell produces a small bud which then grows. When mitosis and cytokinesis are complete, the bud detaches to form the new daughter cell. This budding leaves a scar on the surface of the cell. Therefore, it is possible to count the number of cell divisions that a particular yeast cell has undergone by counting the number of budscars. We imitate this process in our model and keep track of the number of divisions by the introduction of a dummy species, *budscar*, which increases by one, every time the cell passes from M to G1 phase. The reaction and equation for the budscar species are shown in appendix A.

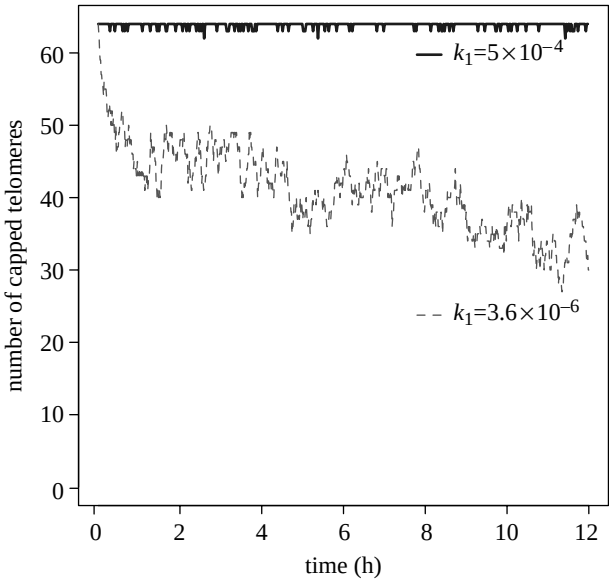

Figure 3. Model predictions of the number of capped telomeres in a wild-type cell when $k_1 = 3.6\times10^{-6}$ or $k_1 = 0.0005$. The output is for one simulation over a period of 12 h.

2.3. Initial conditions and parameter values

Before a model can be simulated, the initial amount of each species must be specified.

We obtained values for the majority of the initial amounts of proteins by consulting the yeast green fluorescent protein (GFP) fusion localization database (http://yeastgfp.ucsf.edu; Huh *et al.* 2003). We assume that initially all the checkpoint proteins are in their inactive state. In the G2 phase of the cell cycle, budding yeast contains 32 chromosomes and so have 64 telomeres, which we assume are all initially bound by Cdc13. We do not include detail of DNA replication in our model and so assume that the total number of telomeres is constant. Table 1 lists all the species, their respective initial amounts, the systematic names of all genes and the database terms so that each entity can be identified in public accessible bioinformatics databases.

The rate constants for each of the reactions are listed in table 2. Note that the value of k_1 was set at 5×10^{-4}, although we had calculated it to be 3.6×10^{-6} from published data (Lin *et al.* 2001), a 100- fold difference. This is because with our original value of k_1, we found that the binding of Cdc13 to telomeres was not strong enough to keep them in a capped state (figure 3). Our model suggests that the binding of Cdc13 to telomeres must be stronger *in vivo* and it is probably the case that the binding affinity of Cdc13 is increased when it is in complex with Stn1 and Ten1 (Grandin *et al.* 2001*b*). At present, there are no experimental data to support this, but it seems a reasonable assumption. Therefore, we increased the value of k_1 until we obtained results in which telomeres only become uncapped transiently as in figure 3 and chose $k_1 = 0.0005$ as our default value. Figure 4 shows the model predictions for the kinetics of uncapping for the *cdc13-1* strain when placed at the

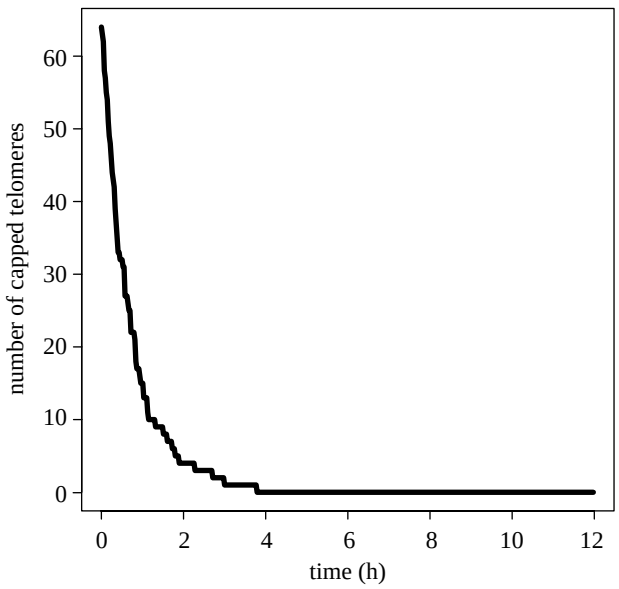

Figure 4. Model predictions for the kinetics of uncapping in the *cdc13-1* strain at the restrictive temperature (with the default parameters). The output is for one simulation over a period of 12 h.

restrictive temperature using the default parameters. The only other kinetic data currently available for parameterizing the model are rates of single strand production in *cdc13-1* mutants at high temperatures, where a rate of 8 kb h^{-1} has been observed (Jia *et al.* 2004; Zubko *et al.* 2004). The actual rates for the different nucleases are unknown, but they were chosen to reflect the suggested relative difference; therefore, we assumed that ExoX activity is 10 times faster than Exo1 activity.

We created an initial computer representation of the model using estimates for parameter values taken directly from evidence in the literature, where available. In some cases, parameter values started as initial best guesses. This initial model was then simulated and the results compared to experimental data. The parameter values were then adjusted to ensure that the model complied with that data. We are confident that the adjustments made to parameters were either to parameters for which we did not have specific data or that the data was derived from *in vitro* experiments, which do not necessarily correspond to the *in vivo* conditions of the culture experiments.

We coded the models in the systems biology markup language (SBML) level 2 (Hucka *et al.* 2003). SBML is a way of representing biochemical networks and is one of the standards used by the modelling community. It has been evolving since mid-2000 through the efforts of an international group of software developers and users. The models were developed using MATHSBML (Shapiro *et al.* 2004). The final model for the wild-type cell was encoded using SBML shorthand and then converted into full SBML (Wilkinson 2006). The model was then imported into the biology of ageing e-science integration and simulation (BASIS) system (www.basis.ncl.ac.uk) and the models for mutant strains were created by making simple modifications to the original model.

To simulate the model, we used a stochastic simulator based on the Gillespie algorithm (Gillespie 1977), since many of the processes being modelled occur at random times. This means that different outcomes may result from the same set of initial conditions. In addition, some of the species in our model must be considered as discrete units rather than continuous variables. For example, species representing the number of capped and uncapped telomeres must be a small integer and so it is not appropriate to use a deterministic simulator for this model. However, we also tried running simulations with a deterministic simulator to see if any parts of the model could be successfully modelled this way (see §3.3). The stochastic simulations were carried out on a Linux Beowulf cluster and the results were stored in a database. All the models and results in this paper are obtainable from the BASIS website (www.basis.ncl.ac.uk). For further details, see Gillespie *et al.* (2006*a*,b). The model for the wild-type strain, where cell death is included, is also available from the Biomodels database (ID:MODEL8679489165) at http://www.ebi.ac.uk/biomodels/ (Le Novère *et al.* 2006).

We did not carry out a full sensitivity analysis for the model parameters, since this would have been very time consuming due to the number of parameters and the fact that we used a stochastic simulator. However, many of the model parameters were chosen after many trials with different values and so it is possible to discuss the effects of changing these. The checkpoint response is sensitive to changes by an order of magnitude to the values of the parameters for the rate of capping (k_1) and Rad17 binding to uncapped telomeres (k_3). A 10-fold decrease in k_1 or a 10-fold increase in k_3 leads to an overactivation of the checkpoint response. The parameters involved in nuclease activity and removal of ssDNA were confined within fairly limited ranges in order to obtain rates of ssDNA production observed in *cdc13-1* mutant strains. The parameters for cell-cycle arrest (k_{15} and k_{16}) could be increased with less effect on the model predictions, but lowering the values led to an unsustained cell-cycle arrest, which could easily be overcome by Cdk activity. The rate of Rad9 activation (k_9) was the most important parameter in the checkpoint pathway and affected not only how quickly the cell responded once the threshold level of ssDNA was reached, but also how quickly nuclease activity was inhibited. The other parameters in the checkpoint response had no significant effect on the model predictions for the rate of ssDNA production or the number of divisions before cell-cycle arrest or cell death. For example, a 10-fold increase or decrease on the rate of Mec1 binding (parameter k_{8d}) did not change the rate of ssDNA production, the total level of ssDNA or the number of divisions before cell-cycle arrest.

3. RESULTS

3.1. Wild-type cells

The model predicts that capped telomeres may become transiently uncapped, but are then recapped. At any time, there is usually only one uncapped telomere at the

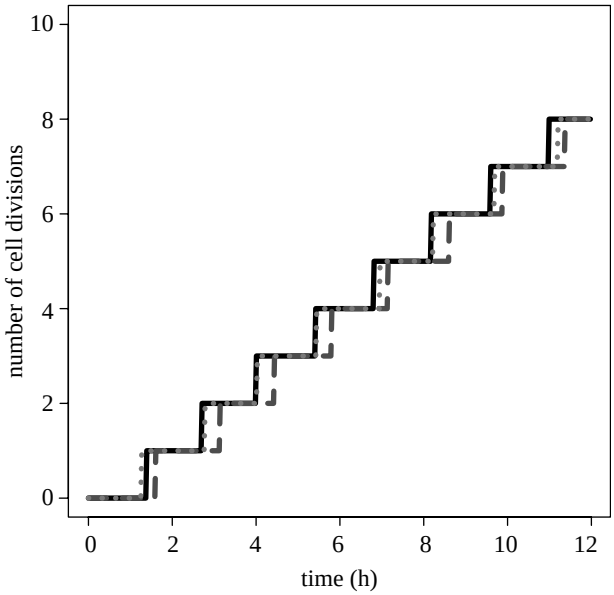

Figure 5. Model predictions for the number of divisions obtained in a wild-type cell. The output is for three simulations over a period of 12 h.

most, but on occasions, two or three telomeres may be uncapped simultaneously (figure 3). However, they do not remain uncapped long enough for Rad17 to bind, so very little ssDNA is produced (data not shown). Figure 5 shows the model predictions for the number of divisions obtained in three different simulation runs. Since we have used a stochastic simulator, each run produces a slightly different output. The cells divide *ca* 7–9 times in a period of 12 h, which gives an average division time of *ca* 1.5 h. This corresponds to the division time obtained when wild-type cells are grown at the restrictive temperature.

3.2. cdc13-1 *mutant strains*

3.2.1. Cell divisions. We used our model to simulate *cdc13-1* mutant strains at the restrictive temperature by setting the initial amount of Cdc13=0, Ctelo=0 and Utelo=64. We can also examine the effects of knocking out different genes for checkpoint proteins and nucleases. For example, to simulate a *cdc13-1 rad9Δ* strain, we set the initial amount of Rad9I=0 (see table 4). Our model predicts that *cdc13-1* cells are unable to divide, although occasionally they may divide once before cell-cycle arrest occurs (data not shown). This is due to the uncapped telomeres being bound by Rad17, which then initiates a series of events leading to cell-cycle arrest. Both Rad9 and Rad24 are required for cell-cycle arrest to occur. Our model predicts that *cdc13-1 exo1Δ* double mutants enter cell-cycle arrest after a few divisions as ssDNA can still be produced through the activity of ExoX and so Rad9 is activated, and in turn, the other checkpoint proteins are activated. The later activation of the checkpoint response is due to the slower generation of ssDNA without the activity of Exo1. Figure 6 shows data from Zubko *et al.* (2004) for various yeast strains cultured at the restrictive temperature. The *cdc13-1* mutants are unable to divide at the restrictive temperature, but

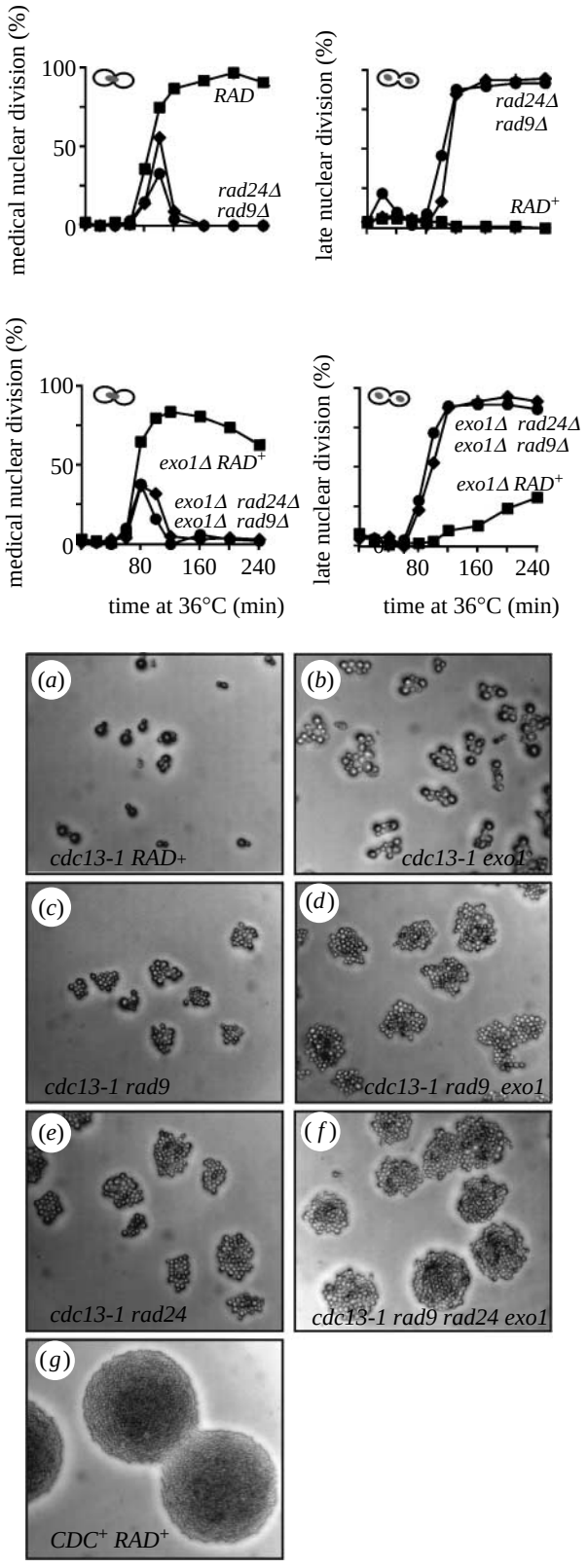

Figure 6. Growth of wild-type and *cdc13-1* mutant strains (reproduced with permission from Zubko *et al.* (2004); Copyright Genetics Society of America). Yeast strains were released from G1 arrest and allowed to form microcolonies for 15 h at 36°C (restrictive temperature) before being photographed at 200× magnification. Cell numbers within microcolonies were estimated from the photographs shown and are given, along with their standard deviations, for each strain: (*a*) *cdc13-1 RAD+*(2); (*b*) *cdc13-1 exo1* (8±2); (*c*) *cdc13-1 rad9* (18±5); (*d*) *cdc13-1 rad9 ex01* (54±17); (*e*) *cdc13-1 rad24* (43±22); (*f*) *cdc13-1 rad9 rad24 exo1* (113±34); (*g*) wild type.

knocking out Rad24, Rad9 or Exo1 restores cell division, hence microcolonies form. Both *cdc13-1 rad9Δ* and *cdc13-1 exo1Δ* double mutants at the restrictive temperature have very small microcolonies, although we know that knocking out Rad9 would prevent cell-cycle arrest (figure 6). The cells for *cdc13-1 exo1Δ* strain are larger than in the *cdc13-1 rad9Δ* strain, which indicates that cells initially arrest and then eventually escape this arrest and divide a few times before cell death takes place. The *cdc13-1* strains accumulate large amounts of ssDNA, since nuclease activity is intact and this is probably the cause of cell death. If we compare the model output with experimental data, we see good agreement apart from the *cdc13-1 rad9Δ* mutant. Our model predicts that *cdc13-1 rad9Δ* cells keep dividing, but experimental data show that these cells only form very small microcolonies (figure 6). This is because we had not included the possibility of cell death in the model. To take cell death into account, we modified the model (see §3.2.3). Our model also does not fit the observation of cell-cycle arrest followed by escape for the *cdc13-1 exo1Δ* strain as we have not included this mechanism in the model. We outline a possible extension to include this escape mechanism in §4.

3.2.2. Generation of ssDNA. Zubko *et al.* (2004) showed that large amounts of ssDNA are produced in *cdc13-1* mutants at the restrictive temperature, but that deleting Exo1 considerably reduced these levels. Deleting Rad24 also reduced the amount of ssDNA, but deleting Rad9 had the opposite effect (see Zubko *et al.* 2004). Therefore, we plotted the level of ssDNA at different time points for each of the different mutant strains and compared our results to Zubko *et al.*'s (2004) data.

Our models predict that initially large amounts of ssDNA are generated in *cdc13-1* strains (figure 7), but this stabilizes when cells enter G2/M arrest, as nuclease activity is inhibited by Rad9 and Rad53. Large amounts of ssDNA are generated in *cdc13-1 rad9Δ* double mutants, since Rad9 is required to inhibit nuclease activity. In contrast, only small amounts of ssDNA are generated in *cdc13-1 rad24Δ* double mutants. This is due to the fact that in our model Rad24 is required to load Rad17 onto uncapped telomeres and so activate ExoX. Our model predicts that much lower levels of ssDNA are generated in *cdc13-1 exo1Δ* double mutants than in the *cdc13-1* strain. This low level of ssDNA is due to the residual activity of ExoX, which has not been completely inhibited by Rad9. The generation of ssDNA in the *cdc13-1 rad24Δ* strain is due to the Rad24-independent activity of Exo1 and the difference between the amount of ssDNA in the *cdc13-1* strain and the *cdc13-1 exo1Δ* strain reflects the total activity of Exo1. Since experimental data show that this difference is larger than the amount of ssDNA generated in the *cdc13-1 rad24Δ* strain (Zubko *et al.* 2004), we suggest that there is also some additional Rad24-independent activation of Exo1 and so have included this in the model. Note that our model does not distinguish between different regions of the telomeres and that the model output represents the total amount of

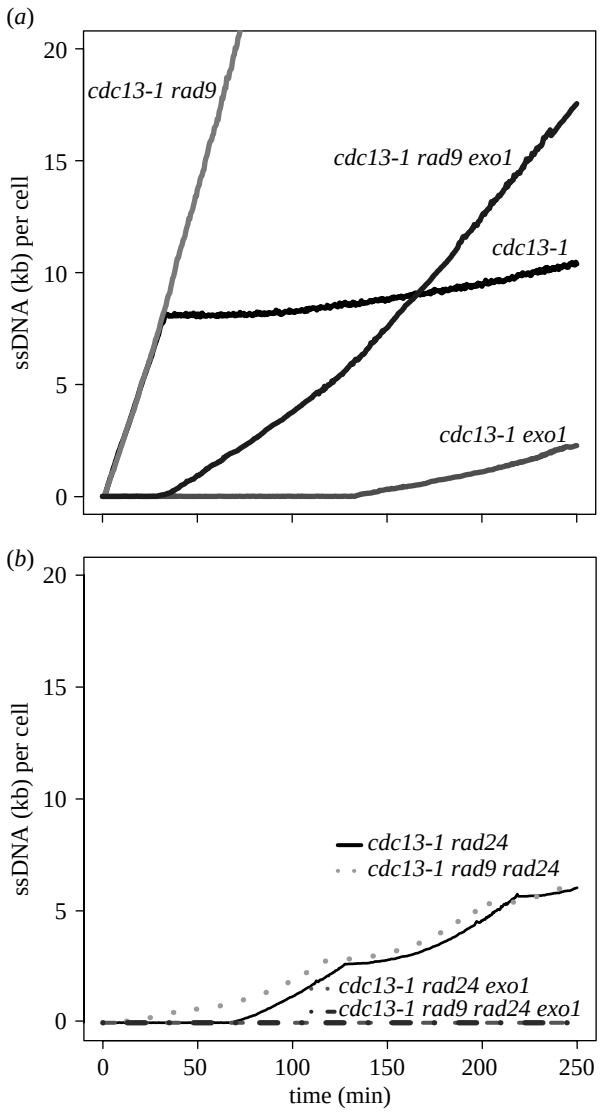

Figure 7. Model predictions for the amount of ssDNA generated in wild-type and *cdc13-1* mutant strains. The output is for one simulation for each strain over a period of 250 min.

ssDNA for all telomeres. To examine the effects of nuclease activity at different regions of the telomere, we would need to modify the model to include a separate species for each telomere and separate reactions for different parts of the telomere.

We also looked at the variability of the amount of ssDNA produced over repeated simulations. We found that the variation from run to run was very small and even with 10 simulations, the upper and the lower 95% confidence interval for the mean was always within 2% of the mean. Therefore, it was not necessary to carry out many repeated simulations.

3.2.3. Extending the model to include cell death. When *cdc13-1 rad9Δ* cells are cultured at the restrictive temperature, it has been found that despite the lack of Rad9, which is required to activate the checkpoint pathway, these cells only divide for a few hours and then die (Zubko *et al.* 2004). The death of cells is due to the large amounts of ssDNA generated in these mutants. Therefore, we modified our model to allow

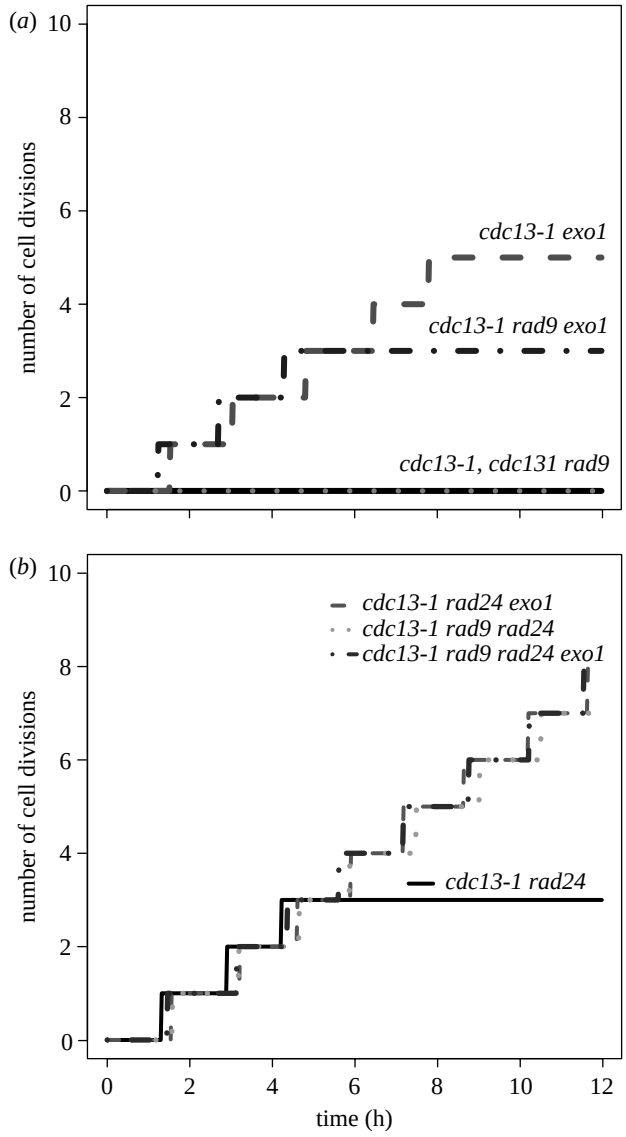

Figure 8. Model predictions for the number of divisions obtained by wild-type and *cdc13-1* mutant strains if a critical threshold of 20 kb ssDNA triggers cell death. The output is for one simulation for each strain over a period of 12 h.

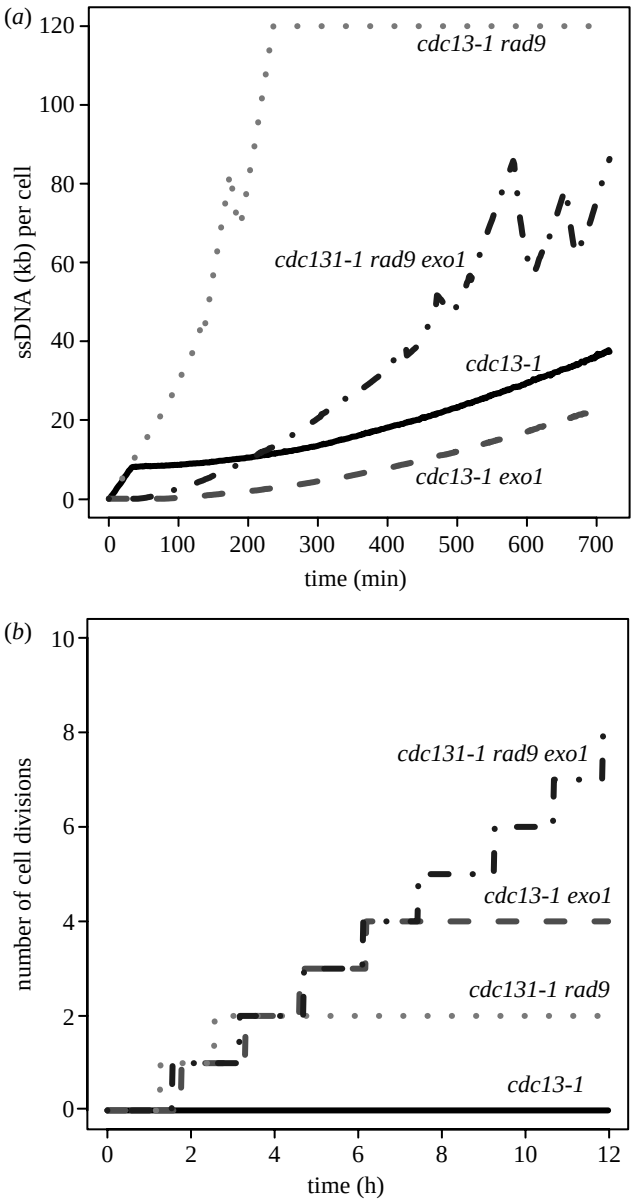

Figure 9. Model predictions for (*a*) the amount of ssDNA per cell and (*b*) the number of cell divisions if a critical threshold of 120 kb ssDNA triggers cell death. The output is for one simulation for each strain over a period of 12 h.

for the possibility of cell death if the total ssDNA for the cell reached a critical threshold of 20 kb. There is currently no data on the amount of ssDNA required to trigger cell death, but it has been observed that there is *ca* 15 kb ssDNA present in *cdc13-1 exo1Δ* strains (Zubko *et al.* 2004). Hence, assumed that the threshold must be greater than this and initially chose 20 kb. The results for this model are in figure 8 and the model now predicts that the *cdc13-1 rad9Δ* cells do not divide since the critical threshold of ssDNA for cell death is reached before it is time to divide (figure 9*a*). Therefore, we increased the critical threshold for cell death to 120 kb and this allows the *cdc13-1 rad9Δ* cells to divide two to three times before cell death (figure 9*b*). These results agree much better with the experimental data, since the *cdc13-1 rad9Δ exo1Δ* cells are able to form larger microcolonies than both *cdc13-1 rad9Δ* cells and *cdc13-1 exo1Δ* cells (figure 6).

However, with this increased threshold, the model predicts that *cdc13-1 rad9Δ exo1Δ* cells are able to keep dividing as in the absence of Exo1, the rate of single strand production is lower and since these cells are dividing, ssDNA can be removed during S phase. This accounts for the zig-zag line in figure 9*a*. Since the rate of ssDNA removal depends on the level of ssDNA, there comes a point at which there is a balance between the rate of generation and removal of DNA. For the *cdc13-1 rad9Δ exo1Δ* cells, this balance occurs somewhere between 60 and 80 kb. This suggests that the threshold for cell death might not be as high as 120 kb, but somewhere in the region of 60–80 kb. Therefore, we did further simulations with a critical threshold of 70 kb. In this case, the model predicts that *cdc13-1 rad9Δ exo1Δ* cells divide 6–7 times, *cdc13-1 exo1Δ* cells divide 3–5 times, *cdc13-1 rad9Δ* cells divide just once and *cdc13-1* cells do not divide at all (data not shown).

Simulations were also carried out for *rad53Δ* and *mec1Δ* mutant strains. We found lower rates of ssDNA production in both *cdc13-1 rad53Δ exo1Δ* and *cdc13-1*

mec1Δexo1Δ strains than in *cdc13-exo1Δ*strains, which agrees with experimental data (Jia *et al.* 2004) This ssDNA was the result of ExoX activity, which was not completely inhibited by Rad9. Our models predicted that the rate of ssDNA production was less than 1 kb h^{-1} on an average for both the strains (data not shown).

Table 4 summarizes all the knockout experiments performed and compares the model predictions with the experimental data. Where agreement is not close, a suggestion for modifying the model has been made.

3.3. Deterministic versus stochastic simulation

We also used a deterministic simulator to run the model to examine whether any parts of the model could be successfully modelled using an ordinary-differential-equation (ODE) framework. We found that the generation of ssDNA could be modelled in this way, and the output for the amount of ssDNA is very similar using either a deterministic or stochastic simulator. This is because the variation in the amount of ssDNA for a number of stochastic simulations was small and typically large numbers were involved. However, information was lost for other parts of the model when using a deterministic simulator. For example, in the wild-type model, the deterministic output for the number of capped and uncapped telomeres gave a steady state of 63.85 and 0.15, respectively, which reflects the average number of capped and uncapped telomeres at any point in time, whereas output from the stochastic simulator show the exact numbers of capped and uncapped telomeres at any time point. Similarly, the number of divisions obtained by *cdc13-1* mutant strains in a stochastic simulation was generally low integers and showed some variability, whereas the deterministic output could only show the average value. The advantage of using deterministic models is the greater speed of simulation and so it is worth considering the usage of a hybrid approach, where parts of the model are simulated using a deterministic simulator and other parts (e.g. low-copy number species) are simulated with a stochastic simulator. There are also hybrid simulators being developed, which combine exact stochastic with approximate stochastic algorithms. Further details of hybrid simulation can be found in Kiehl *et al.* (2004) and Wilkinson (2006).

4. DISCUSSION

We have developed a mathematical model of the yeast checkpoint response, which has been successfully used to test ideas about the checkpoint response to telomere uncapping in budding yeast. The model was modified and used to predict the behaviour of *cdc13-1* cells at the restrictive temperature, and in addition, we carried out simulations, where one or more genes were deleted. We compared simulation output to experimental data of the amount of ssDNA generated over time and the number of cell divisions obtained for the different mutant strains. Generally, we found good agreement with our model predictions and the schema in figure 1. We found that it was necessary to include cell death in the model and that the model output depends on the assumption made about the critical threshold of ssDNA for cell death. This has been useful to discover and suggests that further experimental work is needed to determine this threshold. To explain the experimental observation that *cdc13-1 exo1Δ* initially stops dividing and then escapes from cell-cycle arrest, it will be necessary to extend the model to include the mechanism of adaptation (discussed later).

The models have been kept as simple as possible while retaining enough biological realism and provide the starting point for further investigation. They were encoded in SBML, hence they can easily be extended at any point in the network. For example, it is a fairly easy task to add in further proteins that are involved in the network such as the MRX complex (Mre11, Rad50 and Xrs2), which may be involved in processing telomeric ends and in telomere capping (Larrivee *et al.* 2004; Foster *et al.* 2006). Another protein complex, important at telomeres, is the Yku70/Yku80 heterodimer, which has a similar role to Cdc13 in binding telomere ends and protecting them from repair and checkpoint pathways (Maringele & Lydall 2002). An important kinase which we have not yet included in the model is the Tel1 kinase. Takata *et al.* (2004) show that Tel1 and Mec1 are recruited reciprocally to telomeres during the cell cycle. Tel1 is recruited to telomeres with a repressive structure and is needed to prevent telomeres from fusing through non-homologous end joining in collaboration with telomerase. Mec1 associates preferentially with shortened telomeres during replication. Our model could be modified to investigate this process.

It might also be desirable to add in further details about some of the proteins that are already in the model. For example, Rad9 functions as an 859 kDa complex in undamaged cells, but undergoes a conformational change in the presence of DNA damage (Gilbert *et al.* 2001). This change involves loss of mass and hyperphosphorylation and requires the essential chaperones, Ssa1 and Ssa2 (Gilbert *et al.* 2003). Another example is Mec1, which not only is recruited to damaged DNA, but also resides at the telomeres even in the absence of damage (Takata *et al.* 2004). This might affect the kinetics of RPA recruitment to ssDNA and therefore it requires further investigation. Interestingly, a recent study shows that the cell-cycle kinase Cdk1 is required for the recruitment of ssDNA-binding complex, RPA and that it is also involved in degradation, which occurs at double-stranded DNA breaks (Ira *et al.* 2004). There is no direct evidence that it is involved in the degradation of ssDNA at telomeres, but it would be interesting to see how adding the requirement for Cdk1 to allow RPA-binding affects the model predictions.

Further details of the telomere end protection pathway could also be incorporated into the model. For example, a recent study by Verdun *et al.* (2005) found that telomeres are unprotected during the G2 phase of the cell cycle and that a localized DNA damage response at telomeres after replication is essential for recruiting the processing machinery that promotes formation of a chromosome end protection complex. Since our model incorporates the cell cycle, it would be fairly straightforward to add this extra detail to the model.

JOURNAL OF THE ROYAL SOCIETY Interface
JOURNAL OF THE ROYAL SOCIETY Interface

Table 4. Summary table of knockout simulations for *cdc13-1* strains (model with cell death).

gene(s) knocked out	initial conditions specific for knockout	behaviour predicted by model	experimental results	comparison of predictions with data	suggested improvement to model (where required)	references
rad9	Rad9I=0	0–1 divisions[a] *ca* 20 kb ssDNA after 1 h	3–5 divisions[b] very high levels of ssDNA	model predicts less divisions than observed	increase threshold of ssDNA for cell death (see figure 9)	Zubko *et al.* (2004)
exo1	Exo1I=0	1–5 divisions *ca* 3 kb ssDNA after 4 h	1–4 divisions low levels of ssDNA	good agreement	Add mechanism of adaptation	Zubko *et al.* (2004)
rad9, exo1	Rad9I=0, Exo1I=0	1–4 divisions *ca* 20 kb ssDNA after 6 h	2–7 divisions high levels of ssDNA	model predicts less divisions than observed	increase threshold of ssDNA for cell death (see figure 9)	Zubko *et al.* (2004)
rad24	Rad24=0	3–5 divisions *ca* 6 kb ssDNA after 6 h	0–7 divisions low levels of ssDNA	good agreement	n.a.[c]	Zubko *et al.* (2004)
rad24, exo1	Rad24=0, Exo1I=0	no cell arrest no ssDNA	no cell arrest very low levels of ssDNA	good agreement	n.a.	Zubko *et al.* (2004)
rad9, rad24	Rad9I=0, Rad24=0	no cell arrest *ca* 6 kb after 6 h	no cell arrest low levels of ssDNA	good agreement	n.a.	Zubko *et al.* (2004)
rad9, rad24, exo1	Rad9I=0, Rad24=0, Exo1I=0	no cell arrest no ssDNA	no cell arrest very low levels of ssDNA	good agreement	n.a.	Zubko *et al.* (2004)
rad53, exo1	Rad53I=0 Exo1I=0	*ca* 3 kb ssDNA after 4 h	low levels of ssDNA	good agreement	n.a.	Jia *et al.* (2004)
mec1, exo1	Mec1=0 Exo1I=0	*ca* 3 kb ssDNA after 4 h	low levels of ssDNA	good agreement	n.a.	Jia *et al.* (2004)

[a] Predicted number of divisions in a 15 h period.
[b] Number of divisions per cell in a 15 h period, estimated from the mean and standard deviation of colony size as given in Zubko *et al.* (2004).
[c] n.a., not applicable.

A less straightforward, but by no means impossible, task is to replace the pool of telomeres with individual telomeres to allow the investigation of telomere dynamics. The easiest way to do this would be to have an array or a set of telomere species in the model. Currently, SBML does not support models with arrays or sets, but proposals have been put forward to incorporate this feature into SBML level 3 (www.sbml.org). The model could then be used to investigate the action of telomerase and the possibility that either abrupt shortening or lengthening may cause cell-cycle arrest (Ijpma & Greider 2003; Viscardi *et al.* 2003). To examine the effects of nuclease activity at different regions of the telomere (Zubko *et al.* 2004), we would need additionally to add separate reactions for different parts of the telomere and keep track of the amount of ssDNA acquired in the different regions. This would be very interesting to do and the model could then be used to test the hypotheses that different nucleases are important at different regions of the telomeres (Zubko *et al.* 2004).

We could also modify our model so that it is possible to carry out simulations, which involve changing the temperature of *cdc13-1* mutant strains. A simple way to do this is to add two variables to the model to represent the permissive and restrictive temperature, e.g. Temp23 and Temp36. At the permissive temperature, Temp23 and Temp36 are set to 1 and 0, respectively, and at the restrictive temperature, the settings are reversed. The addition of Temp23 to the kinetic law of the capping reaction would ensure that this reaction could only proceed at the permissive temperature (if Temp23 = 0, then the rate of the reaction would also be 0 and so unable to take place). The temperature could be switched at certain time points during the course of the simulation to mimic the experimental procedure of moving cells from the permissive temperature to the restrictive temperature and vice versa.

Experimental data shows that the function of *cdc13-1* is totally disrupted at 36°C (Garvik *et al.* 1995). As the temperature is lowered, *cdc13-1* function is gradually restored so that there is a positive correlation between function and decreasing temperature (Zubko *et al.* 2004). We could model this scenario by having a species in the model to represent the temperature, e.g. Temp, and to choose a kinetic law so that the rate of the capping reaction depends on the value of Temp. The value of Temp could be changed at different time points during the simulation to mimic the experimental procedure of switching temperatures.

The cells for *cdc13-1 exo1Δ* strain are larger than in the *cdc13-1 rad9Δ* strain, which indicates that cells initially arrest and then eventually escape this arrest and divide an average of three times before cell death takes place (figure 6; Zubko *et al.* 2004). Our model predicts that the *cdc13-1 exo1Δ* strain divide four or five times and then arrest. Therefore, it is desirable to add the possibility of escape from cell arrest into the model. It is known that escape (also known as adaptation) from cell arrest occurs even though the damage and the signal for damage persists and that the time for escape is *ca* 8–15 h (Toczyski *et al.* 1997; Gardner *et al.* 1999; Pellicioli *et al.* 2001). Studies have shown that escape requires the proteins Cdc5 and casein kinase II (Toczyski *et al.* 1997) and that Rad53 kinase activity and Chk1 phosphorylation largely disappear at the time that cells escape arrest, provided functional Cdc5 is present (Pellicioli *et al.* 2001). Cdc5 is a target of Rad53, and phosphorylation of Cdc5 is required for the completion of anaphase (Sanchez *et al.* 1999). Pellicioli *et al.* (2001) suggest that Cdc5 acts in a feedback loop to turn off the checkpoint kinase cascade, but at present we do not know the exact mechanism of how this is achieved. Trying to model this scenario would help to clarify the details of this pathway.

The models in this paper have followed the fate of one individual cell. It would be interesting to extend the models to follow an entire colony. This would be much more computer intensive to do, but should become easier in the future as computing power continues to increase. The addition of arrays or sets into SBML would also make it much easier to code population-based models.

Finally, the models developed in this paper were motivated by hypotheses put forward as a result of experimental work. Our models do not preclude the possibility that other hypotheses may also be able to explain the experimental results. Therefore, we strongly encourage the interested reader to either make their own modifications to the models or to send us their suggestions so that other ideas can be tested.

This work was funded by BBSRC, MRC, EPSRC, DTI and Unilever plc. D.L. is also funded by the Wellcome Trust. We thank three anonymous referees for their very helpful suggestions.

APPENDIX A. MODELLING THE CELL CYCLE

We model the cell cycle by having a species for each of its stages: G1, S, G2 and M.

Initially G1 = 1 and S = G2 = M = 0, which means that the cell is in G1 phase. When the cell goes into S phase, G1 = 0, S = 1 and so on.

Each phase of the cycle is governed by the growth of a cyclin, which must reach a sufficient level before it will bind and activate a protein kinase Cdk. When the Cdk is activated, it signals for the transcription of genes necessary for the transition into the next stage of the cell cycle. When these genes have been transcribed, the cycle can proceed to the next stage. Cyclins are continually degraded, but only synthesized during the phase to which they are related. This can be modelled by a set of biochemical reactions and an event, which triggers the activation of the Cdk when the cyclin reaches a threshold level. The reactions and event for the G2 to M phase transition are listed below (all the other reactions are easily written down by replacing G2 with M and M with G1 to get the reactions for the M to G1 transition and so on).

$$\mathrm{G2} \xrightarrow{k_{c1}} \mathrm{G2} + \mathrm{G2cyclin},$$

$$\text{If } \mathrm{G2cyclin} > 100, \text{ then } \mathrm{G2CdkA} = 1, \mathrm{G2CdkI} = 0,$$

$$\mathrm{G2Moff} + \mathrm{G2} + \mathrm{G2CdkA} \xrightarrow{k_{c2}} \mathrm{G2Mon} + \mathrm{G2} + \mathrm{G2CdkA},$$

$$\mathrm{G2cyclin} \xrightarrow{k_{c3}} \sin k,$$

$$\mathrm{G2} + \mathrm{G2CdkA} + \mathrm{G2Mon} \xrightarrow{k_{c4}} \mathrm{M} + \mathrm{G2CdkI} + \mathrm{G2Moff}.$$

Table A1. Identifiers and initial conditions for cell cycle.

species	description	systematic name[a] (for genes)	database term[b]	initial value (no. of molecules)
G1	G1 phase	n.a.[c]	GO:0051318	1
S	S	n.a.	GO:0000084	0
G2	G2	n.a.	GO:0051319	0
M	M	n.a.	GO:0000279	0
G1cyclin	G1 cyclin	YMR199W	S000004812	0
Scyclin	S cyclin	YPR120C	S000006324	0
G2cyclin	G2 cyclin	YPR119W	S000006323	0
Mcyclin	M cyclin	YGR108W	S000003340	0
G1CdkI	inactive Cdk	YBR160W	S000000364	0
G1CdkA	active Cdk	YBR160W	S000000364	0
SCdkI	inactive Cdk	YBR160W	S000000364	0
SCdkA	active Cdk	YBR160W	S000000364	0
G2CdkI	inactive Cdk	YBR160W	S000000364	0
G2CdkA	active Cdk	YBR160W	S000000364	0
MCdkI	inactive Cdk	YBR160W	S000000364	0
MCdkA	active Cdk	YBR160W	S000000364	0
G1Soff	G1 to S transition off	n.a.	GO:0000082	1
G1Son	G1 to S transition on	n.a.	GO:0000082	0
SG2off	S to G2 transition off	n.a.	GO:0000115	1
SG2on	S to G2 transition on	n.a.	GO:0000115	0
G2Moff	G2 to M transition off	n.a.	GO:0031572	1
G2Mon	G2 to M transition on	n.a.	GO:0000086	0
MG1off	M to G1 transition off	n.a.	GO:0000087	1
MG1on	M to G1 transition on	n.a.	GO:0000087	0
budscar	scar on membrane for each division	n.a.	n.a.	0

[a] Systematic names (or ORF-name) corresponds to stretch of DNA of the sequenced gene.
[b] Database terms starting with: (i) GO are taken from the Gene Ontology database (www.geneontology.org); (ii) S are taken from the *Saccharomyces* Genome Database (www.yeastgenome.org).
[c] n.a., not applicable.

Table A2. Reactions for the cell cycle.

reaction	kinetic rate law	reactants	products	parameter	value[a]
G1 cyclin synthesis	k_{c1}[G1]	G1	G1, G1cyclin	k_{c1}	0.16 s^{-1}
S cyclin synthesis	k_{c1}[S]	S	S, Scyclin	k_{c1}	0.16 s^{-1}
G2 cyclin synthesis	k_{c1}[G2]	G2	G2, G2cyclin	k_{c1}	0.16 s^{-1}
M cyclin synthesis	k_{c1}[M]	M	M, Mcyclin	k_{c1}	0.16 s^{-1}
G1 to S genes on	k_{c2}[G1][G1Soff][G1CdkA]	G1, G1Soff, G1CdkA	G1, G1Son, G1CdkA	k_{c2}	0.01 $mol^{-2}\,s^{-1}$
S to G2 genes on	k_{c2}[S][SG2off][SCdkA]	S, SG2off, SCdkA	S, SG2on, SCdkA	k_{c2}	0.01 $mol^{-2}\,s^{-1}$
G2 to M genes on	k_{c2}[G2][G2Moff][G2CdkA]	G2, G2Moff, G2CdkA	G2, G2Mon, G2CdkA	k_{c2}	0.01 $mol^{-2}\,s^{-1}$
M to G1 genes on	k_{c2}[M][MG1off][MCdkA]	M, MG1off, MCdkA	M, MG1on, MCdkA	k_{c2}	0.01 $mol^{-2}\,s^{-1}$
G1 cyclin degradation	k_{c3} [G1cyclin]	G1cyclin	sink	k_{c3}	0.0012 s^{-1}
S cyclin degradation	k_{c3}[Scyclin]	Scyclin	sink	k_{c3}	0.0012 s^{-1}
G2 cyclin degradation	k_{c3}[G2cyclin]	G2cyclin	sink	k_{c3}	0.0012 s^{-1}
M cyclin degradation	k_{c3}[Mcyclin]	Mcyclin	sink	k_{c3}	0.0012 s^{-1}
G1 to S progression	k_{c4}[G1][G1CdkA][G1Son]	G1, G1CdkA, G1Son	S, G1CdkI, G1Soff	k_{c4}	0.01 $mol^{-2}\,s^{-1}$
S to G2 progression	k_{c4}[S][SCdkA][SG2on]	S, SCdkA, SG2on	G2, SCdkI, SG2off	k_{c4}	0.01 $mol^{-2}\,s^{-1}$
G2 to M progression	k_{c4}[G2][G2CdkA][G2Mon]	G2, G2CdkA, G2Mon	M, G2CdkI, G2Moff	k_{c4}	0.01 $mol^{-2}\,s^{-1}$
M to G1 progression	k_{c4}[M][MCdkA][MG1on]	M, MCdkA, MG1on	G1, MCdkI, MG1off, budscar	k_{c4}	0.01 $mol^{-2}\,s^{-1}$

[a] mol = number of molecules.

Table A3. List of events affecting cell cycle.

event	trigger	species affected	reactions affected
G1Cdk activation	G1cyclin > 100	G1CdkA, G1CdkI	G1 to S genes on, G1 to S progression
SCdk activation	Scyclin > 100	SCdkA, SCdkI	S to G2 genes on, S to G2 progression
G2Cdk activation	G2cyclin > 100	G2CdkA, G2CdkI	G2 to M genes on, G2 to M progression
MCdk activation	Mcyclin > 100	MCdkA, MCdkI	M to G1 genes on, M to G1 progression

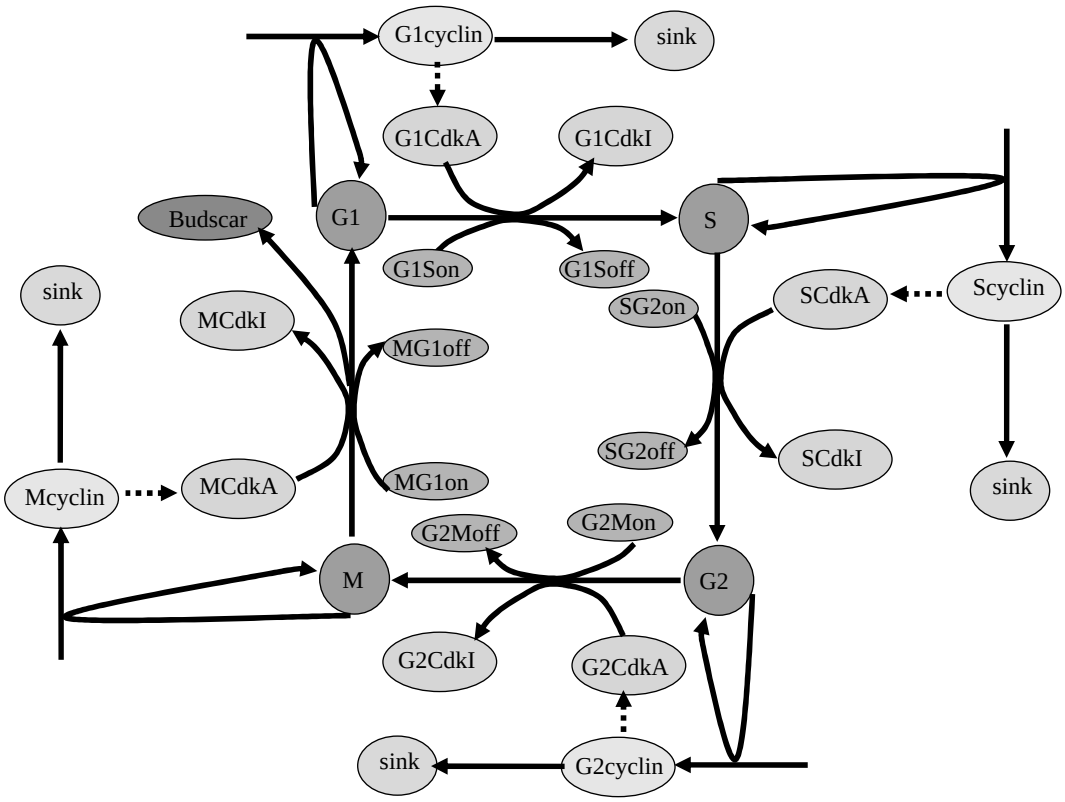

Figure A1. Network diagram of the cell-cycle model. G1CdkA and G1CdkI represent the active and inactive G1 Cdk, respectively, and similarly for the other Cdks. The dashed lines connecting the cyclins to the Cdks indicate events. When a cyclin reaches a level of 100, the respective Cdk is activated.

G2CdkI represents the inactive kinase and G2CdkA represents the active form. The first line is the reaction for the synthesis of the G2 cyclin; the second line gives the event which triggers activation of the G2 Cdk; the third line is the reaction for the transcription of genes required for G2 to M phase transition; the fourth line is the reaction for cyclin degradation and the last line is the reaction which results in the transition from G2 to M phase. The parameter values chosen were $k_{c1}=0.16$, $k_{c2}=0.01$, $k_{c3}=0.0012$ and $k_{c4}=0.01$. With these values, each phase lasts *ca* 20 min. Initially, all the Cdks are in their inactive state (G2CdkI = 1, G2CdkA = 0, etc.), all cell-cycle genes are off (G2Moff = 1, G2Mon = 0, etc.) and the level of each cyclin is 0.

To keep track of the number of cell divisions made by an individual cell, a dummy species called budscar was introduced which increased by 1 every time the cell cycle progressed from the M phase to G1. This was represented by the following reaction:

$$\mathrm{M} + \mathrm{MG1on} + \mathrm{MCdkA} \xrightarrow{k_{c4}} \mathrm{G1} + \mathrm{MG1off} + \mathrm{MCdkI} + \mathrm{budscar}.$$

The rate law for this equation is k_{c4}[#M][#MG1on][#MCdkA] and since the species M, MG1on and MCdkA can only take the value 1 or 0, the reaction can only proceed when all of M, MG1on and MCdkA are equal to 1.

A complete list of the species used in modelling the cell cycle, the initial amounts, the systematic names for the genes and database terms are given in table A1. A complete list of reactions and events are given in tables A2 and A3, respectively, and figure A1 shows the complete network for the cell-cycle model.

REFERENCES

Blankley, R. T. & Lydall, D. 2004 A domain of Rad9 specifically required for activation of Chk1 in budding yeast. *J. Cell Sci.* **117**, 601–608. (doi:10.1242/jcs.00907)

Foster, S. S., Zubko, M. K., Guillard, S. & Lydall, D. 2006 MRX protects telomeric DNA at uncapped telomeres of budding yeast *cdc13-1* mutants. *DNA Repair* **5**, 840–851.

Gardner, R., Putnam, C. W. & Weinert, T. 1999 RAD53, DUN1 and PDS1 define two parallel G(2)/M checkpoint pathways in budding yeast. *EMBO J.* **18**, 3173–3185. (doi:10.1093/emboj/18.11.3173)

Garvik, B., Carson, M. & Hartwell, L. 1995 Single-stranded DNA arising at telomeres in *cdc13* mutants may constitute a specific signal for the Rad9 checkpoint. *Mol. Cell. Biol.* **15**, 6128–6138.

Gilbert, C. S., Green, C. M. & Lowndes, N. F. 2001 Budding yeast Rad9 is an ATP-dependent Rad53 activating machine. *Mol. Cell* **8**, 129–136. (doi:10.1016/S1097-2765(01)00267-2)

Gilbert, C. S., van den Bosch, M., Green, C. M., Vialard, J. E., Grenon, M., Erdjument-Bromage, H., Tempst, P. & Lowndes, N. F. 2003 The budding yeast Rad9 checkpoint complex: chaperone proteins are required for its function. *EMBO Rep.* **4**, 1–6. (doi:10.1038/sj.embor.embor935)

Gillespie, D. T. 1977 Exact stochastic simulation of coupled chemical reactions. *J. Phys. Chem.* **31**, 2340–2361. (doi:10.1021/j100540a008)

Gillespie, C. S., Wilkinson, D. J., Proctor, C. J., Shanley, D. P., Boys, R. J. & Kirkwood, T. B. L. 2006*a* Tools for the SBML community. *Bioinformatics* **22**, 628–629. (doi:10.1093/bioinformatics/btk042)

Gillespie, C. S., Wilkinson, D. J., Shanley, D. P., Proctor, C. J., Boys, R. J. & Kirkwood, T. B. L. 2006*b* BASIS: an internet resource for network modelling. *J. Integr. Bioinformatics* **3**(2), 26. See http://journal.imbio.de/index.php?paper_id=26.

Grandin, N., Damon, C. & Charbonneau, M. 2001*a* Cdc13 prevents telomere uncapping and Rad50-dependent homologous recombination. *EMBO J.* **20**, 6127–6139. (doi:10.1093/emboj/20.21.6127)

Grandin, N., Damon, C. & Charbonneau, M. 2001*b* Ten1 functions in telomere end protection and length regulation in association with Stn1 and Cdc13. *EMBO J.* **20**, 1173–1183. (doi:10.1093/emboj/20.5.1173)

Hucka, M., Finney, A., Sauro, H. M., Bolouri, H., Doyle, J. C. & Kitano, H. 2003 The systems biology markup language (SBML): a medium for representation and exchange of biochemical network models. *Bioinformatics* **19**, 524–531. (doi:10.1093/bioinformatics/btg015)

Huh, W. K., Falvo, J. V., Gerke, L. C., Carroll, A. S., Howson, R. W., Weissman, J. S. & O'Shea, E. K. 2003 Global analysis of protein localization in budding yeast. *Nature* **425**, 686–691. (doi:10.1038/nature02026)

Ijpma, A. S. & Greider, C. W. 2003 Short telomeres induce a DNA damage response in *Saccharomyces cerevisiae*. *Mol. Biol. Cell* **14**, 987–1001. (doi:10.1091/mbc.02-04-0057)

Ira, G. *et al.* 2004 DNA end resection, homologous recombination and DNA damage checkpoint activation require CDK1. *Nature* **431**, 1011–1017.

Jia, X. D., Weinert, T. & Lydall, D. 2004 Mec1 and Rad53 inhibit formation of single-stranded DNA at telomeres of *Saccharomyces cerevisiae* cdc13-1 mutants. *Genetics* **166**, 753–764. (doi:10.1534/genetics.166.2.753)

Kiehl, T. R., Mattheyses, R. M. & Simmons, M. K. 2004 Hybrid simulation of cellular behavior. *Bioinformatics* **20**, 316–322. (doi:10.1093/bioinformatics/btg409)

Larrivee, M., LeBel, C. & Wellinger, R. J. 2004 The generation of proper constitutive G-tails on yeast telomeres is dependent on the MRX complex. *Genes Dev.* **18**, 1391–1396. (doi:10.1101/gad.1199404)

Le Novère, N. *et al.* 2006 Biomodels database: a free, centralized database of curated, published, quantitative kinetic models of biochemical and cellular systems. *Nucleic Acids Res.* **34**, D689–D691. (doi:10.1093/nar/gkj092)

Lin, Y. C., Hsu, C. L., Shih, J. W. & Lin, J. J. 2001 Specific binding of single-stranded telomeric DNA by Cdc13p of *Saccharomyces cerevisiae*. *J. Biol. Chem.* **276**, 24 588–24 593. (doi:10.1074/jbc.M101642200)

Lydall, D. 2003 Hiding at the ends of yeast chromosomes: telomeres, nucleases and checkpoint pathways. *J. Cell Sci.* **116**, 4057–4065. (doi:10.1242/jcs.00765)

Lydall, D. & Weinert, T. 1995 Yeast checkpoint genes in DNA damage processing: implications for repair and arrest. *Science* **270**, 1488–1491.

Majka, J. & Burgers, P. M. J. 2003 Yeast Rad17/Mec3/Cdc1: a sliding clamp for the DNA damage checkpoint. *Proc. Natl Acad. Sci. USA* **100**, 2249–2254. (doi:10.1073/pnas.0437148100)

Maringele, L. & Lydall, D. 2002 EXO1-dependent single-stranded DNA at telomeres activates subsets of DNA damage and spindle checkpoint pathways in budding yeast yku70 Delta mutants. *Genes Dev.* **16**, 1919–1933. (doi:10.1101/gad.225102)

Maringele, L. & Lydall, D. 2005 The PAL-mechanism of chromosome maintenance-causes and consequences. *Cell Cycle* **4**, 747–751.

Pellicioli, A., Lee, S. B., Lucca, C., Foiani, M. & Haber, J. E. 2001 Regulation of *Saccharomyces* Rad53 checkpoint kinase during adaptation from DNA damage-induced G2/M arrest. *Mol. Cell* **7**, 293–300. (doi:10.1016/S1097-2765(01)00177-0)

Sanchez, Y., Bachant, J., Wang, H., Hu, F. H., Liu, D., Tetzlaff, M. & Elledge, S. J. 1999 Control of the DNA damage checkpoint by Chk1 and Rad53 protein kinases through distinct mechanisms. *Science* **286**, 1166–1171. (doi:10.1126/science.286.5442.1166)

Schwartz, M. F., Duong, J. K., Sun, Z., Morrow, J. S., Pradhan, D. & Stern, D. F. 2002 Rad9 phosphorylation sites couple Rad53 to the *Saccharomyces cerevisiae* DNA damage checkpoint. *Mol. Cell* **9**, 1055–1065. (doi:10.1016/S1097-2765(02)00532-4)

Shapiro, B. E., Hucka, M., Finney, A. & Doyle, J. 2004 MathSBML: a package for manipulating SBML-based biological models. *Bioinformatics* **20**, 2829–2831. (doi:10.1093/bioinformatics/bth271)

Takata, H., Kanoh, Y., Gunge, N., Shirahige, K. & Matsuura, A. 2004 Reciprocal association of the budding yeast ATM-related proteins Tel1 and Mec1 with telomeres in vivo. *Mol. Cell* **14**, 515–522. (doi:10.1016/S1097-2765(04)00262-X)

Toczyski, D. P., Galgoczy, D. J. & Hartwell, L. H. 1997 CDC5 and CKII control adaptation to the yeast DNA damage checkpoint. *Cell* **90**, 1097–1106. (doi:10.1016/S0092-8674(00)80375-X)

Vaze, M. B., Pellicioli, A., Lee, S. E., Ira, G., Liberi, G., Arbel-Eden, A., Foiani, M. & Haber, J. E. 2002 Recovery from checkpoint-mediated arrest after repair of a double-strand break requires Srs2 helicase. *Mol. Cell* **10**, 373–385. (doi:10.1016/S1097-2765(02)00593-2)

Verdun, R. E., Crabbe, L., Haggblom, C. & Karlseder, J. 2005 Functional human telomeres are recognized as DNA damage in G2 of the cell cycle. *Mol. Cell* **20**, 551–561. (doi:10.1016/j.molcel.2005.09.024)

Viscardi, V., Baroni, E., Romano, M., Lucchini, G. & Longhese, M. P. 2003 Sudden telomere lengthening triggers a Rad53-dependent checkpoint in *Saccharomyces cerevisiae*. *Mol. Biol. Cell* **14**, 3126–3143. (doi:10.1091/mbc.E02-11-0719)

Weinert, T. A. & Hartwell, L. H. 1988 The Rad9 gene controls the cell cycle response to DNA damage in *Saccharomyces cerevisiae*. *Science* **241**, 317–322.

Wilkinson, D. J. 2006 *Stochastic modelling for systems biology*. Boca Raton, FL: Chapman & Hall/CRC Press.

Zou, L. & Elledge, S. J. 2003 Sensing DNA damage through ATRIP recognition of RPA-ssDNA complexes. *Science* **300**, 1542–1548. (doi:10.1126/science.1083430)

Zubko, M. K., Guillard, S. & Lydall, D. 2004 Exo1 and Rad24 differentially regulate generation of ssDNA at telomeres of *Saccharomyces cerevisiae* cdc13-1 mutants. *Genetics* **168**, 103–115. (doi:10.1534/genetics.104.027904)